APEM journal

Advances in Production Engineering & Management
Volume 15 | Number 2 | June 2020 | pp 164–178
https://doi.org/10.14743/apem2020.2.356

ISSN 1854-6250
Journal home: apem-journal.org
Original scientific paper

Development of family of artificial neural networks for the prediction of cutting tool condition

Spaić, O.[a]**, Krivokapić, Z.**[b]**, Kramar, D.**[c,*]

[a]University in East Sarajevo, Faculty of Production and Management Trebinje, Bosnia and Herzegovina
[b]University in Montenegro, Faculty of Mechanical Engineering Podgorica, Montenegro
[c]University in Ljubljana, Faculty of Mechanical Engineering Ljubljana, Slovenia

ABSTRACT

Recently, besides regression analysis, artificial neural networks (ANNs) are increasingly used to predict the state of tools. Nevertheless, simulations trained by cutting modes, material type and the method of sharpening twist drills (TD) and the drilling length from sharp to blunt as input parameters and axial drilling force and torque as output ANN parameters did not achieve the expected results. Therefore, in this paper a family of artificial neural networks (FANN) was developed to predict the axial force and drilling torque as a function of a number of influencing factors. The formation of the FANN took place in three phases, in each phase the neural networks formed were trained by drilling lengths until the drill bit was worn out and by a variable parameter, while the combinations of the other influencing parameters were taken as constant values. The results of the prediction obtained by applying the FANN were compared with the results obtained by regression analysis at the points of experimental results. The comparison confirmed that the FANN can be used as a very reliable method for predicting tool condition.

ARTICLE INFO

Keywords:
Drilling;
Cutting tool;
Twist drill bits;
Axial force;
Tool wear;
Prediction;
Artificial neural networks;
Back propagation

**Corresponding author:*
davorin.kramar@fs.uni-lj.si
(Kramar, D.)

Article history:
Received 8 January 2020
Revised 24 June 2020
Accepted 27 June 2020

1. Introduction

The prediction of the tool condition, i.e. the determination of correlations between the target function and the influencing parameters, is of high importance, since the technological and economic effects of the machining process depend directly on the tool life. However, due to the highly complex phenomena that develop within the cutting zone and are caused by the influence of a number of mutually collinear factors, modeling the cutting process is difficult. One of the most accurate and reliable methods for predicting the tool condition is the experimental-analytical method, in which a regression model for predicting the tool condition is created on the basis of the determined dependence of the target function on the influencing parameters [1]. Nevertheless, regression analysis does not provide satisfactory results when the relationship between the target function and the influencing parameters is non-linear, as is usually the case in cutting, and requires additional experiments. For this reason, many researchers have recently started to apply the principles of ANNs to the modeling of the cutting process.

Krivokapić *et al*. [2], explored the possibility of using ANN to predict the wear of S390 high speed steel twist drills (TD) produced by powder metallurgy (PM), when drilling hardened steel. TD nominal diameter, sharpening mode, number of revolutions, feed rate and drilling length were used as input parameters and the mean value of the wear band width of the back surface was used as output parameter. Kaya *et al*. [3] presented an effective and efficient model for assessing cutting tool wear when milling the Inconel 718 superalloy, based on ANN. The model trained with components of cutting force in three axes, torque, conditions and cutting time showed a very good correlation between actual and predicted values of tool wear. Also in milling operations, Wu *et al*. [4] compared three machine learning algorithms, including ANNs, SVR, and RFs in predicting tool wear. Performance measures include mean square error, R square, and training time. A number of statistical characteristics have been extracted from cutting forces, vibrations, and acoustic emissions. A similar study using a Response Surface Methodology (RSM), a genetic algorithm (GA) and a Grey Wolf Optimizer (GWO) algorithm to predict surface roughness in ball-end nose milling of hardened steel was conducted by Sekulic *et al*. [5]. Two modeling techniques, RSM and ANN, have been used to develop R_a and *VB* predictive models in turning and their predictive capabilities have been compared in a study by Tamang *et al*. [6]. Netoa *et al*. [7] used two types of ANN to assess the diameter of precision drilled holes in aluminum and titanium alloys. The input parameters were signals of acoustic emission, power and cutting force and vibration. Rao *et al*. [8] used ANN to predict the surface roughness, the tool wear and the workpiece vibration amplitude drilling AISI 316 steel, and their input parameters were tool tip radius, cutting speed, feed rate and the amount of material removed. The application of ANN [9] resulted in a model for monitoring the wear condition depending on the acoustic emission signal. By applying ANN, Kannan *et al*. [10] have monitored the roughness of the machined surface as a function of the influencing parameters when drilling brass plates and have developed a model for monitoring drill wear with optimisation of feed rate, cutting speed, thrust and torque. Benkedjouh *et al*. [11] formed a model for assessing tool condition and predicting its lifetime, based on the properties obtained from the control signals and the support of vector regression to assess and predict tool wear. Drouillet *et al*. [12] developed an ANN-based model for predicting the remaining tool life based on the value of the measured power of the spindle when milling stainless steel workpieces at different cutting speeds. D'Addona *et al*. [13] showed that ANN is a reliable method for monitoring the wear of drill based on the analysis of vibration signals. Patra *et al*. [14] developed an ANN model to predict the number of drill holes based on axial force, cutting speed, drill spindle speed and feed rate. Khorasani and Yazdi [15] developed a general dynamic ANN system for monitoring surface roughness when milling Al 7075 and St 52 using cutting speed, feed rate, material type, coolant, vibration and noise as input parameters. Mikołajczyk *et al*. [16] confirmed that a useful industrial tool for assessing tool life in turning by combining image recognition software and ANN. Wang and Jia [17] developed ANN to express thrust force and delamination factor as a function of drilling parameters. Multi-objective optimization of drilling parameters is than performed based on NSGA-II. In the research of Kumar and Hynes [18] the ANFIS model has been used for predicting surface roughness of drilled galvanized steel, while optimization was performed using the GA method. In Mondal *et al*. [19] the minization of burr formation in drilling process was performed with the application of regression modeling and ANN. In the work of Schorr *et al*. [20] an approach to predict the quality of drilled and reamed bores was presented. The machine learning method of random forest was used to predict the concentricity and the diameter of the bores on the basis of the torque measurements. Yin *et al*. [21] have established the model by backpropagation ANN for the prediction of microhole diameters and hole roundness in laser drilling.

The importance of predicting tool wear at different cutting conditions, possible limitations of regression analysis and the increasing use of ANN in tool condition prediction were the challenges for this research. The aim of the research was to develop a model for a comprehensive prediction of tool wear of TDs as a function of a number of influencing parameters for drill lengths up to the point when TD became worn. Axial force and torque by drilling were chosen as a target function. Both provide the most reliable information about tool wear that can be measured during the cutting process. The input parameters for ANNs were: the material of the TD, sharpening mode and nominal diameter *d*, number of revolutions *n*, feed rate s and achieved drilling length L_{max}. The attempt to create the desired model by applying a complex ANN did not lead to a satisfactory result; therefore the idea was to form a family of simple ANNs (FANN).

2. Materials and methods

In order to create a model for predicting the TD condition, backpropagation was performed using ANNs. The modeling was based on the determined correlations between the target functions (drilling force and torque) and the influencing parameters by drilling of quenched and tempered alloy steel 42CrMo4 (43-45 HRC). In the experiments, twist drill bits (DIN 338) made of high-speed steel with increased Co content were used, which were produced in the conventional metallurgical process (C) or in the powder metallurgical process (PM), regularly sharpened with a corrected main cutting blade (CMB) or ground crosswise (CL), see Table 1.

The workpiece dimensions (thickness) were adjusted so that the bore length of $L = 3d$ mm is maintained with uniform distribution of the workpiece hardness over the longitudinal and cross section. The cutting conditions were adjusted to the recommendations for drilling hardened steel.

For cooling and lubrication the 8 % solution of Teolin H/VR in the amount of 1 l/min was used. Axial force and torque were measured with the three-component dynamometer "Kistler", TYP 8152B2, in the range from 100 to 900 kHZ, integrated in the conventional drilling machine TYP FGU-32 and connected to a Global Lab software for data acquisition, as illustrated in Fig. 1. The initial experiment was conducted with four repetitions of drilling tests in the central point according to the matrix plan for three-factor experiment shown in Table 2.

Table 1 Tool material and sharpening modes for TDs

Influential parameters	
Cutting tool material	High-speed steel with 8 % Co, produced in conventional metallurgy process, S2-9-1-8, (C)
	High-speed steel with 8 % Co, produced in powder metallurgy, S390 MICROCLEAN, (PM)
Sharpening mode of drills	Regular with corrected main blade (CMB)
	Cross-like (CL)

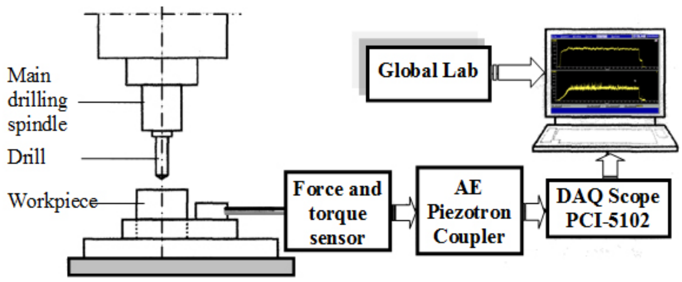

Fig. 1 Set-up for measurement of axial force and torque in drilling [1]

Table 2 Matrix plan of three-factor experiment [1]

Experimental points	Coded values			Real values			Output vectors
	x_1	x_2	x_3	d [mm]	n [rpm]	s [mm/rev]	F_a, M
1	-1	-1	-1	6.0	250	0.027	F_1, M_1
2	+1	-1	-1	10.0	250	0.027	F_2, M_2
3	-1	+1	-1	6.0	500	0.027	F_3, M_3
4	+1	+1	-1	10.0	500	0.027	F_4, M_4
5	-1	-1	+1	6.0	250	0.107	F_5, M_5
6	+1	-1	+1	10.0	250	0.107	F_6, M_6
7	-1	+1	+1	6.0	500	0.107	F_7, M_7
8	+1	+1	+1	10.0	500	0.107	F_8, M_8
9	0	0	0	7.75	355	0.053	F_9, M_9
10	0	0	0	7.75	355	0.053	F_{10}, M_{10}
11	0	0	0	7.75	355	0.053	F_{11}, M_{11}
12	0	0	0	7.75	355	0.053	F_{12}, M_{12}

Based on the matrix plan, measurement of the axial force and the torque for the particular experiment was performed at five measuring points for both tool materials and both sharpening modes. The first measurement was performed while drilling $L = 3d$ mm deep holes with sharp

TD, while the fifth measurement was performed when the drilling lengths were reached, whereby the following predefined maximum allowed flank wear values (h_{max}) for different TD were reached:

- for TD Ø6.0 mm – h_{max} = 0.25 mm,
- for TD Ø7.75 mm – h_{max} = 0.30 mm,
- for TD Ø10.0 mm – h_{max} = 0.35 mm.

The other three measurements were performed upon achievement of the drilling lengths whereat the flank wear of TD remained within the interval $0 < h_i < h_{max}$, and i = 2, 3, 4.

Under different experimental conditions (material of TD, sharpening mode, nominal diameter, number of revolutions and feed rate), TD reached the maximum allowed flank wear at different drilling lengths, as shown in Table 3.

Based on the measurement results of all the TD used in the experiments, diagrams for the axial force and the torque as a function of the drilling length and the cutting regime were generated.

Table 3 Drilling lengths at which drills achieved maximum allowable wear

No.	Drills material	Sharpening mode	*d* [mm]	*n* [rpm]	*s* [mm/rev]	L_{max} [mm]	No.	Drills material	Sharpening mode	*d* [mm]	*n* [rpm]	*s* [mm/rev]	L_{max} [mm]
1	S390	CMB	6.0	250	0.027	560	25	S 2-9-1-8	CMB	6.0	250	0.027	630
2			10.0	250	0.027	750	26			10.0	250	0.027	1420
3			6.0	500	0.027	1325	27			6.0	500	0.027	3050
4			10.0	500	0.027	3250	28			10.0	500	0.027	3020
5			6.0	250	0.107	1330	29			6.0	250	0.107	1550
6			10.0	250	0.107	1050	30			10.0	250	0.107	2400
7			6.0	500	0.107	3000	31			6.0	500	0.107	4650
8			10.0	500	0.107	800	32			10.0	500	0.107	720
9			7.75	355	0.053	1730	33			7.75	355	0.053	1755
10			7.75	355	0.053	2370	34			7.75	355	0.053	1220
11			7.75	355	0.053	1920	35			7.75	355	0.053	1520
12			7.75	355	0.053	1870	36			7.75	355	0.053	1480
13		CL	6.0	250	0.027	1300	37		CL	6.0	250	0.027	610
14			10.0	250	0.027	1000	38			10.0	250	0.027	1100
15			6.0	500	0.027	2700	39			6.0	500	0.027	3690
16			10.0	500	0.027	5075	40			10.0	500	0.027	5800
17			6.0	250	0.107	1400	41			6.0	250	0.107	4200
18			10.0	250	0.107	2000	42			10.0	250	0.107	3820
19			6.0	500	0.107	2260	43			6.0	500	0.107	5850
20			10.0	500	0.107	900	44			10.0	500	0.107	800
21			7.75	355	0.053	2650	45			7.75	355	0.053	2750
22			7.75	355	0.053	2530	46			7.75	355	0.053	2340
23			7.75	355	0.053	2650	47			7.75	355	0.053	2400
24			7.75	355	0.053	2850	48			7.75	355	0.053	2440

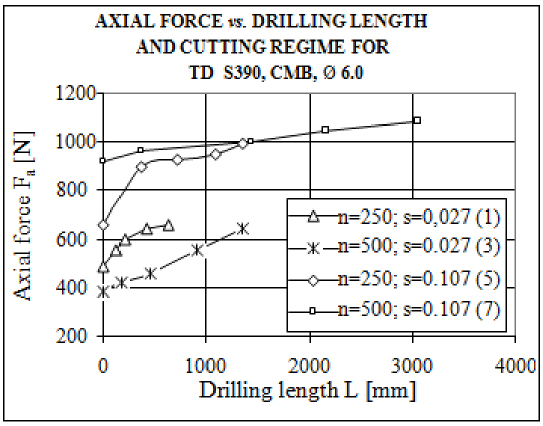

Fig. 2 Axial force *vs.* drilling length and cutting regime for TD S390, CMB, Ø6.0

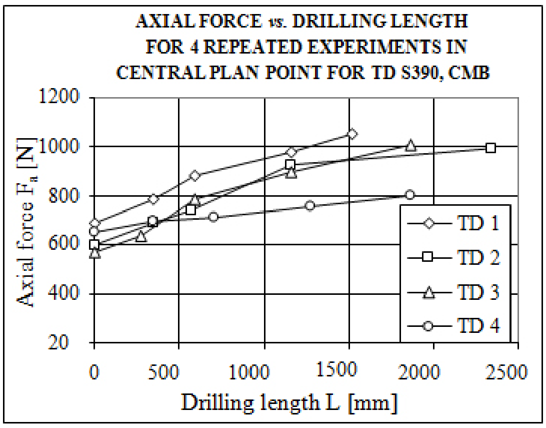

Fig. 3 Axial force *vs.* drilling length for 4 repeated experiments in central plan point (d_4 = 7.75 mm, n_5 = 355 rpm, s_5 = 0.053 mm/rev) for TD S390, CMB

The axial force F_a as a function of the drilling length L for TD Ø6.0 mm, made of S390 PM steel, regularly sharpened (CMB), is shown in Fig. 2 and for TD in the central plan point (d_4 = 7.75 mm, n_5 = 355 rpm, s_5 = 0.053 mm/rev) in Fig. 3. The diagrams show that all the different factors (material of twist drill bits, sharpening mode and cutting regime) had a significant influence on the axial force F_a.

3. Results and discussion

As far as the defined correlation curves are concerned, the trend curves and polynomial equations were defined for their interpretation, thus providing sufficient data sets for the ANN output parameters. After the data research in ANN the tool condition prediction application, a feed-forward back propagation ANN training was conducted in the MATLAB 6.0 software package. The training was performed with six input parameters, three of which were parameters of the cutting regime (nominal diameter d, number of revolutions n, and feed rate s), material type of TD, sharpening mode and drilling length l, and two output parameters – axial drilling force F_a and torque M, as shown in Fig. 4.

What follows is a selection of parameters amongst those offered in back propagation ANN training within MATLAB software package:

1. Training function
2. Adaption learning function
3. Performance function
4. Number of epochs
5. Number of neuron layers, and for each neuron layer
   5.1 Number of neurons in a layer
   5.2 Transfer function

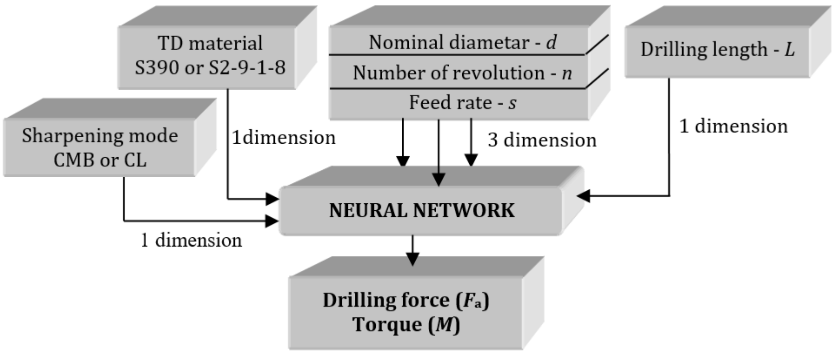

Fig. 4 Complex ANN training scheme [22]

As one of the ways to improve generalization during ANN training, it is suggested to surround each element of the trained family with a low noise level. By applying the above mentioned method, the ANN trainees approached a training error of less than 10^{-10}. After ANN training, it was checked (simulated) with the data relevant to the experiment, but was not used in the training process. However, the simulation of the trainees ANN did not yield the expected results, which indicates that it is impossible to efficiently process a large amount of data for the cutting process using the usual approach with ANN multiple inputs and outputs. This again confirms the fact that predicting the tool condition, which depends on numerous influential parameters, is a delicate matter. The trained ANN had a poor generalization due to the occurrence of the following phenomena:

- depending on the type of TD material, the sharpening mode and the cutting regime (nominal diameter, number of revolutions and feed rate), TD reached the maximum wear at different drilling lengths, as shown in Fig. 2 and Table 3;
- wide dispersion of axial drilling force and torque depending on the type of TD material, sharpening mode and cutting regime; and

- the same type of TD material, the same sharpening mode and the same cutting conditions (nominal diameter, number of revolutions and feed rate) together with different drilling lengths (changing only one of the input parameters while keeping the others constant) are an additional disadvantage for ANN.

3.1 Formation of the family of neural networks (FANN)

Since the trained ANN did not achieve the research goal set for the reasons worked out, the following idea came up: Instead of training a complex ANN with 6 input parameters and axial drilling force F_a and torque M as output parameters, the training of a family of simple ANNs should be carried out with two variable parameters, one of which would always be the drilling length L, while the axial drilling force F_a would be the output parameter.

The formation of a FANN was performed for TD material – PM (high-speed steel produced in powder metallurgy process) and sharpening mode – CBM (regular with corrected main cutting edge), where one of the parameters of the cutting regime (d, n and s) and the drilling length L were variable values, while the combination of the other two parameters was assumed to be constant. As shown in Fig. 5, the formation of FANN (ANNs training) was organised in several phases. In Phase I, the nominal diameter of the TD involved in the experiment (d_1 = 6.0 mm and d_2 = 10.0 mm) and drilling length L were taken as variables, while the combinations of the following parameters involved in the experiment: type of TD material, sharpening mode, number of revolutions and feed rate, were taken as constant values. Over the course of Phase I, simulation of the trained ANN was performed for nominal TD diameters of 6.0 < d_n < 10.0 mm (d_3 = 7.0, d_4 = 7.75 and d_5 = 9.0 mm) and drilling length of L = 0-2.000 mm.

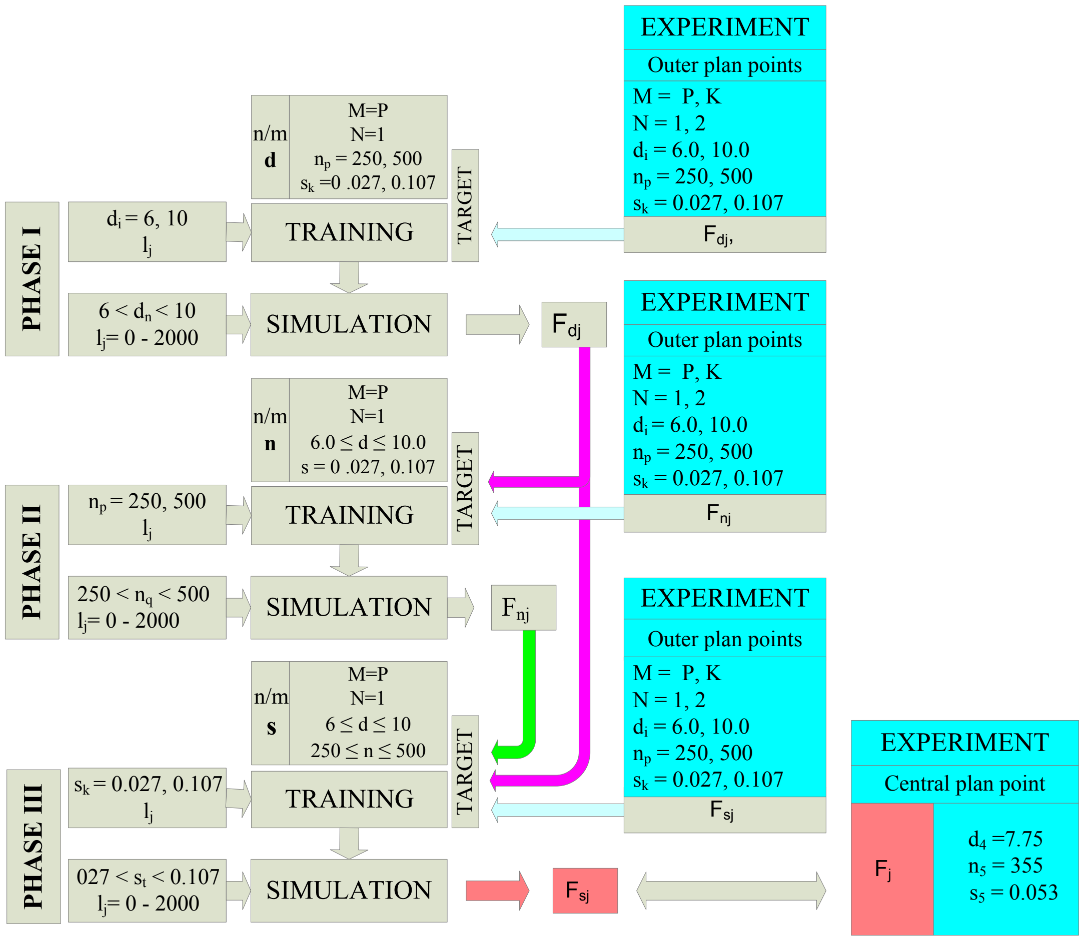

Fig. 5 Development of a family of simple ANNs

During Phase II of ANN formation, values for the number of revolutions n involved in the experiment (n_1 = 250 and n_2 = 500 rpm) and the drilling length L were taken as the variable parameters, while the constant values contained combinations of the following parameters: TD material, sharpening mode and feed rate (s_1 = 0.027 and s_2 = 0.107 mm/rev), and the TD diameters for which the values of the axial forces had been obtained by experimenting and simulating the ANN formed in Phase I (6.0 ≤ d ≤ 10.0 mm). The simulation of ANN in Phase II was performed with the standard number of revolutions within the range 250 < n_q < 500 (n_3 = 280, n_4 = 315, n_5 = 355, n_6 = 400 and n_7 = 450 rpm) and the drilling length L expressed in mm.

In Phase III, values of the feed rate (s_1 = 0.027 and s_2 = 0.107 mm/rev) and the drilling length L were taken as variable parameters, while the constant values comprised combinations of the following parameters: TD material, sharpening mode, diameters within the range of 6.0 ≤ d ≤ 10.0 mm (for which the values of axial force F_a had been obtained by experimenting and simulation of the ANN in Phase I), and standard number of revolutions within the range of 250 ≤ n ≤ 500 rpm (for which the values of axial force F_a had been obtained by experimenting and simulation of the ANN in Phase II). The simulation of a trained ANN in Phase III was performed with the standard feed rate within the interval of 0.027 < s_t < 0.107 (s_3 = 0.033, s_4 = 0.042, s_5 = 0.053, s_6 = 0.067 and s_7 = 0.084 mm/rev) and the drilling length L. The axial drilling force F_a, expressed in N, was chosen as the output parameter of all ANNs.

In Phase I of the FANN formation, only those ANNs were trained which were involved in the experiment with the factor values d_i, n_p and s_k, i.e. the ANN: n11, n21, n12 and n22.

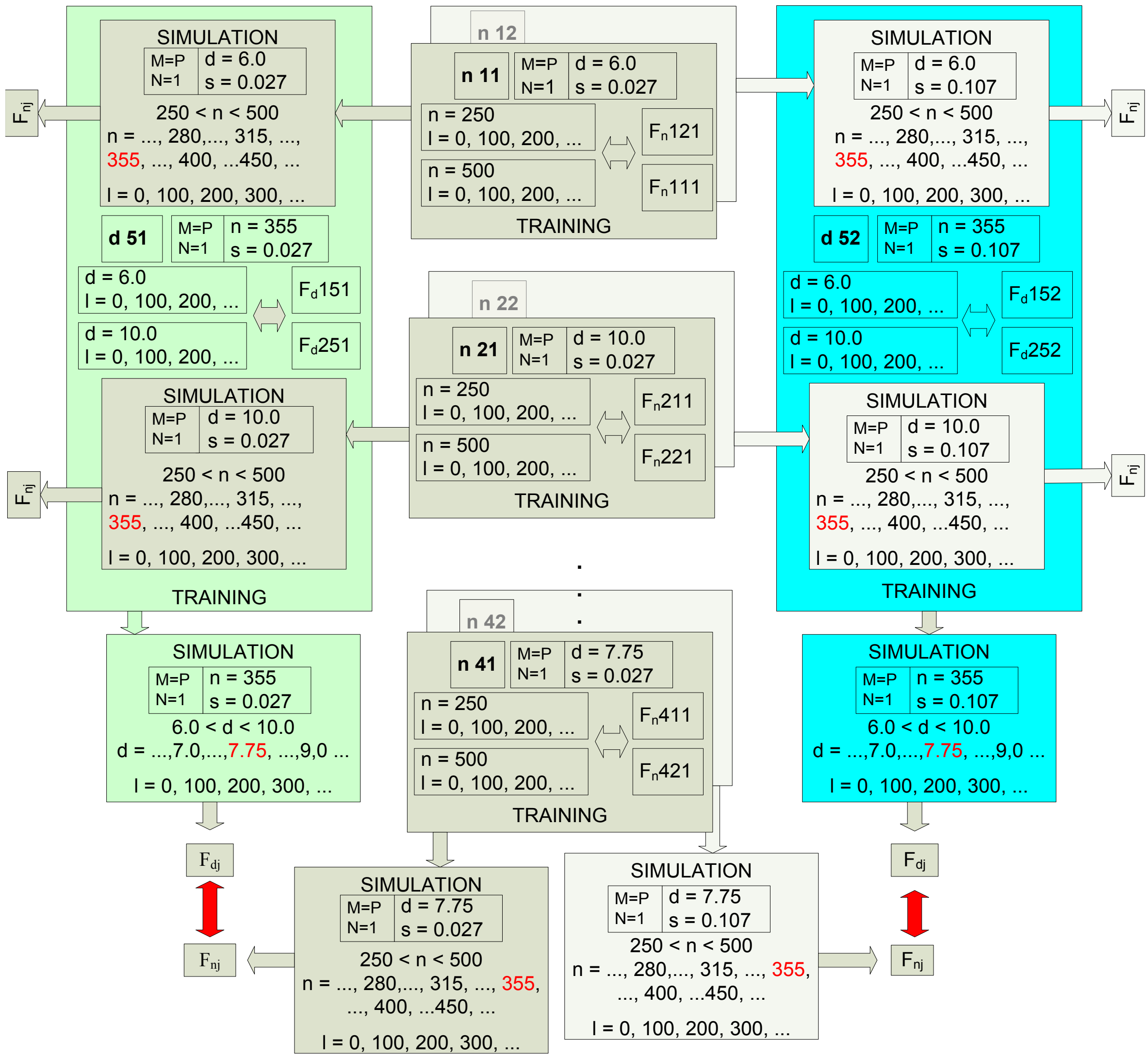

Fig. 6 First model of Phase II of FANN formation

In Phase II, besides the ANN trained with the values of parameters involved in the experiment (n11, n21, n12 and n22), the following ANNs were formed: n41 (n_1 = 250 and n_2 = 500 rpm; d_4 = 7.75 mm; s_1 = 0.027 mm/rev) and n42 (n_1 = 250 and n_2 = 500 rpm; d_4 = 7.75 mm; s_2 = 0.107 mm/rev), as well as control ANNs d51 (d_1 = 6.0 and d_2 = 10.0 mm; n_5 = 355 rpm; s_1 = 0.027 mm/rev) and d52 (d_1 = 6.0 and d_2 = 10.0 mm; n_5 = 355 rpm; s_2 = 0.107 mm/rev), as shown in Fig. 6. The values of the axial force F_a for combinations of influencing parameters of the mentioned ANN were obtained by simulation of ANN in Phase I or by ANN from Phase II, which was trained with the factor values involved in the experiment.

The results of the simulation of ANN n41 for n_5 = 355 rpm (d_4 = 7.75 mm and s_1 = 0.027 mm/rev) shall be consistent with the results of the simulation of control ANN d51 for d_4 = 7.75 mm (n_5 = 355 rpm and s_1 = 0.027 mm/rev), while the results of simulation of ANN n42 for n_5 = 355 rpm shall be consistent with the results of the simulation of the control ANN d52 for d_4 = 7.75 mm.

In Phase III, in addition to the ANNs trained with the factor values involved in the experiment (s11, s21, s12 and s22), the following ANNs were formed: s41 (s_1 = 0.027 and s_2 = 0.107 mm/rev; d_4= 7.75 mm; n_1 = 250 rpm) and s42 (s_1 = 0.027 and s_2 = 0.107 mm/rev; d_4 = 7.75 mm; n_2 = 500 rpm), and the control ANNs d15 (d_1 = 6.0 and d_2 = 10.0 mm; n_1 = 250 rpm; s_5 = 0.053 mm/rev) and d25 (d_1 = 6.0 and d_2 = 10.0 mm; n_2 = 500 rpm; s_5 = 0.053 mm/rev). The values of the axial force F_a for combinations of influencing parameters from the above stated ANNs were obtained by simulating the ANNs from the Phase II, i.e. ANNs of the Phase III which had been trained with the factor values involved in the experiment (s11, s21, s12 and s22). The results of the simulation of ANN s41 for s_5 = 0.053 mm/rev (d_4 = 7.75 mm and n_1 = 250 rpm) must correspond to the results of the simulation of ANN d15 for d_4 = 7.75 mm (n_1 = 250 rpm and s_5 = 0.053 mm/rev), while the results of the simulation of ANN s42 for s_5 = 0.053 mm/rev (d_4 = 7.75 mm and n_2 = 500 rpm) must correspond to those of the simulation of ANN d25 for d_4 = 7.75 mm.

In addition to those ANNs specified in the fifth model in Phase III, the following ANNs were also formed: s15 (s_1 = 0.027 and s_2 = 0.107 mm/rev, d_1 = 6.0 mm and n_5 = 355 rpm), s25 (s_1 = 0.027 and s_2 = 0.107 mm/rev, d_2 = 10.0 mm and n_5 = 355 rpm), s45 (s_1 = 0.027 and s_2 = 0.107 mm/rev; d_4 = 7.75 mm and n_5 = 355 rpm) and control ANNs d55 (d_1 = 6.0 and d_2 = 10.0 mm; n_5 = 355 rpm and s_5 = 0.053 mm/rev) and in the control model also n45 (n_1 = 250 and n_2 = 500 rpm; d_4 = 7.75 mm; s_5 = 0.053 mm/rev), for which the values of the axial force F_a have been obtained by simulating the ANNs from previous phases, as shown in Fig. 7.

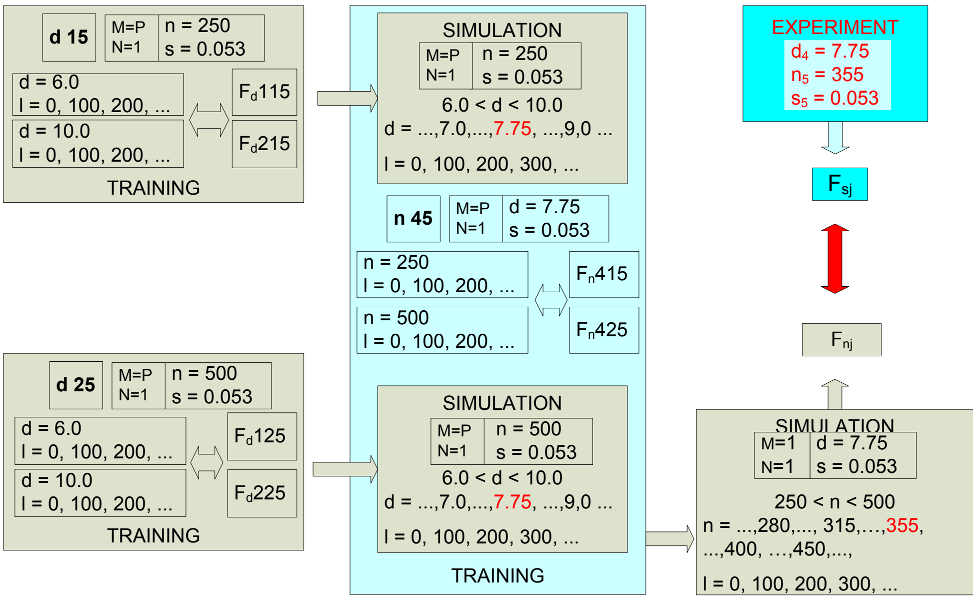

Fig. 7 Control model of FANN formation

Results of the simulation of ANN d55 for d_4 = 7.75 mm (n_5 = 355 rpm, s_5 = 0.053 mm/rev); s45 for s_5 = 0.053 mm/rev (d_4 = 7.75 mm, n_5 =355 355 rpm) and n45 for n_5 = 355 rpm (d_4 = 7.75 mm, s_5 = 0.053 mm/rev) must correspond both to each other and to the results of the experiment in the central plan point (d_4 = 7.75 mm; n_5 = 355 rpm and s_5 = 0.053 mm/rev).

The first training of the ANNs was performed at the outer points of the experiment, using the values of axial force obtained by the experiment as input parameters. The formation of the sequence of ANNs was continued towards the central point of the plan, as shown in Fig. 8, so that the final training was performed in the central point of the plan. As output parameters the values of axial force F_a obtained by the simulation of the ANNs in the previous phases were used.

The values of the axial drilling force F_a as a function of the drilling length and the influencing parameters (type of TD material, sharpening mode, nominal diameter, number of revolutions and feed rate), which were obtained by the simulation of trained ANNs can be graphically displayed, as shown in Figs 9. and 10. Fig. 9. shows the values of the axial force F_a as a function the drilling length obtained by the simulation of ANN d11 (M = PM, SM = CMB, n_1 = 250 rpm, s_1 = 0.027 mm/rev) at the nominal diameters of drills d_3 = 7.0; d_4 = 7.75 and d_5 = 9.0 mm in relation to the values of the axial force determined in the experiment for drills with nominal diameter d_1 = 6.0 and d_2 = 10.0 mm.

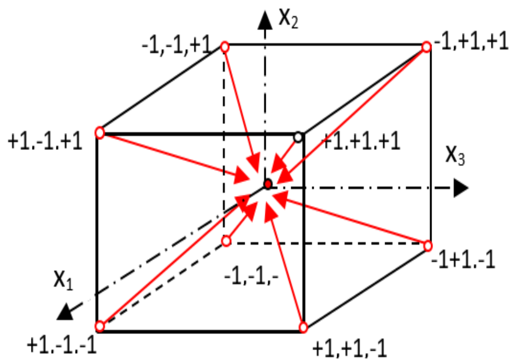

Fig. 8 Direction of development of ANNs

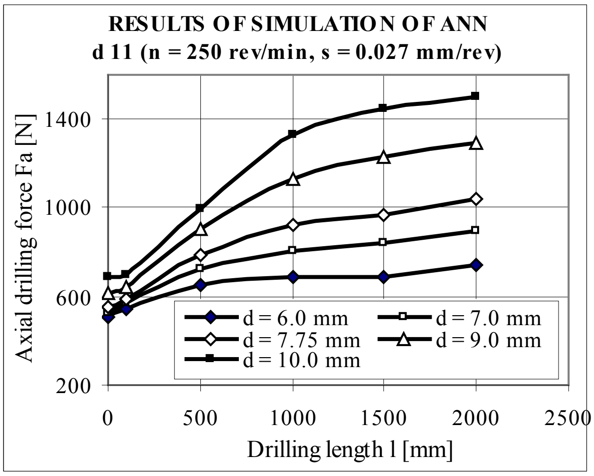

Fig. 9 Results of simulation of ANN d 11 (n_1 = 250 rev/min, s_1 = 0.027 mm/rev)

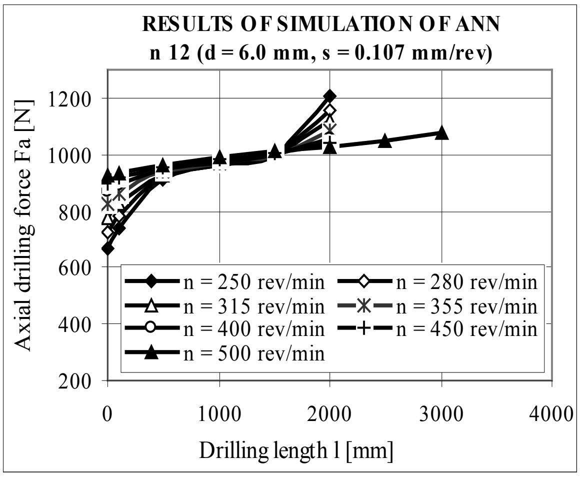

Fig. 10 Results of simulation of ANN n 12 (d_1 = 6.0 mm, s_2 = 0.107 mm/rev)

Fig. 10 shows the values of the axial force F_a as a function of the drilling length obtained by simulating ANN n12 (M = PM, SM = CMB, d_1 = 6.0 rpm, s_2 = 0.107 mm/rev) for the number of revolutions n_3 = 280; n_4 = 315, n_5 = 355, n_6 = 400 and n_7 = 450 rpm, in relation to the value of the axial force at the number of revolutions n_1 = 250 and n_2 = 500 rpm obtained in the experiment. The same principle can be applied to represent the values of axial force as a function of drilling length obtained by simulating others ANNs within the family formed.

Comparison values of the axial drilling force, which were obtained by simulating ANN n41 for n_5 = 355 rpm (d_4 = 7.75 mm, s_1 = 0.027 mm/rev) and control ANN d51 for d_4 = 7.75 mm (n_5 = 355 rpm, s_1 = 0.027 mm/rev) are shown in Fig. 11, while those for ANN s42 for s_5 = 0.053 mm/rev (d_4 = 7.75 mm, n_2 = 500 rpm) and control ANN d25 for d_4 = 7.75 mm (n_2 = 500 rpm, s_5 = 0.053 mm/rev) are shown in Fig. 12. The diagrams show that the results of simulation of control ANN d51 correspond to the results of simulation of ANN n41 with a maximum deviation of 3.14 % for L = 500 mm (Fig. 11), while the results of simulation of control ANN d25 correspond to the results of simulation of ANN s42 with a maximum deviation of 3.95 % for L = 2000 mm (Fig. 12).

The same principle can be used to represent comparative values of axial force obtained by simulation of ANN n42 and control ANN d52 as well as ANN s41 and control ANN d15.

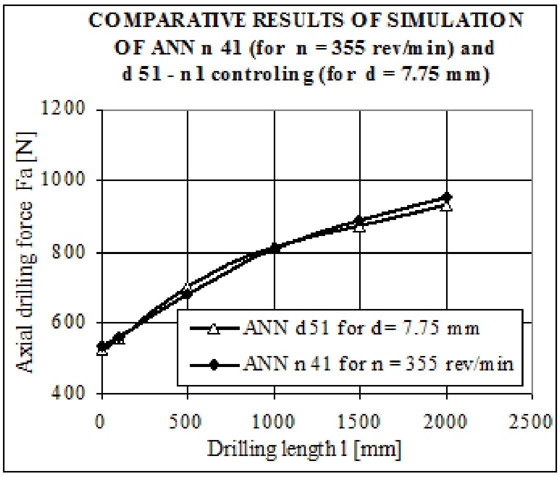

Fig. 11 Comparative results of simulation of ANN n 41 (for n_5 = 355 rpm) and d 51 – n 1 controlling (for d_4 = 7.75 mm)

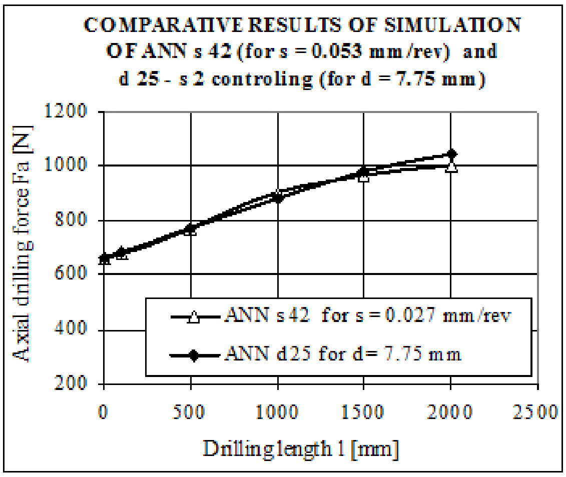

Fig. 12 Comparative results of simulation of ANN s 42 (for s_5 = 0.053 mm/rev) and d 25 – s 2 controlling (for d_4 = 7.75 mm)

The values of the axial drilling force F_a for four repeated experiments in the central plan point and their mean value are shown in Fig. 13. Comparative values of axial drilling force obtained by simulation of ANN s45 for s_5 = 0.053 mm/rev, the control ANN d55 for d_4 = 7.75 mm and n45 for n_5 = 355 rpm, and mean values of the experiments in the central plan point are shown in Fig. 14. The diagrams in Figs 13 and 14 show that the results of the simulation of ANN s45 for s_5 = 0.053 mm/rev and the control ANN d55 for d_4 = 7.75 mm, and n45 for n_5 = 355 rpm correspond to each other and lie within the interval comprising the values of three repeated experimental results in the central plan point.

The results of the fourth repeated experiment deviate both from the results of the other three repeated experiments and from the results obtained by simulating ANN. The comparison of the results of the simulation with the mean value of four experiment results in the central planning point reveals the following:

- the deviation of the results of the simulation of ANN s45 from the mean value of the experimental results is at most 6.598 % for L = 1000 mm;
- the deviation of the results of the simulation of the control ANN d55 from the results of the simulation of ANN s45 is at most 7.89 % for L = 0 mm and from the mean value of the experimental results for four repeated experiments is at most 9.7 % for L = 2000 mm, and
- the deviation of the results of the simulation of the control ANN n45 from the results of the simulation of ANN s45 is maximum 5.596 % and from average of four repeated experiments results maximum of 10.74 % for L = 1000 mm.

The results of the simulation of the ANN central plan point come even closer to the experimental results when compared with the mean value of three instead of all four repeated experiments.

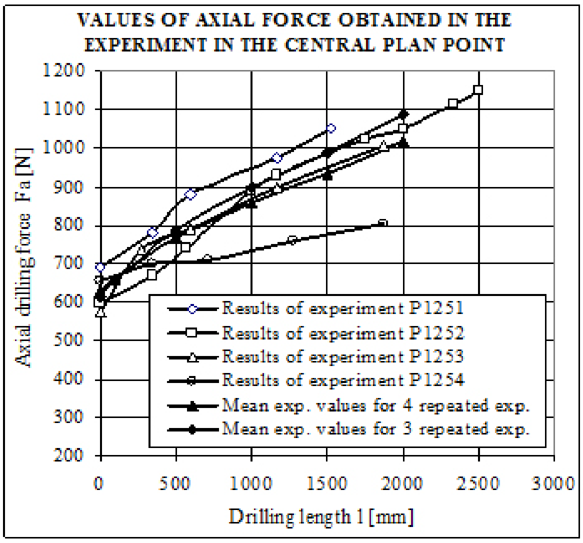

Fig. 13 Value of axial force for four repeated experiments in the central plan point

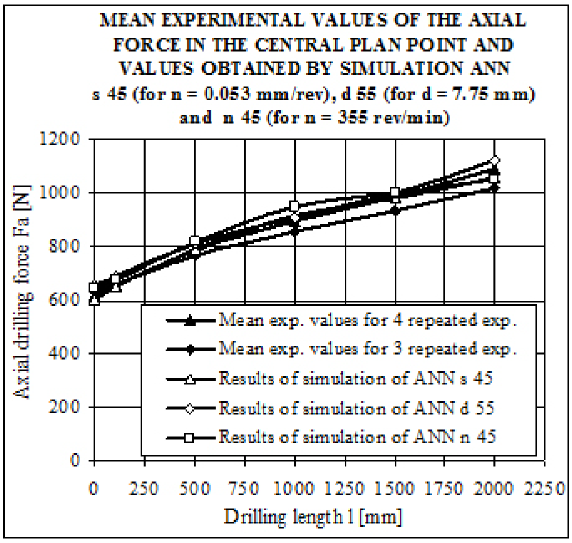

Fig. 14 Comparative values of axial force obtained by simulation of ANN s 45 (for s_5 = 0.053 mm/rev), d 55 (for d_4 =7.75 mm) and n 45 (for n_5 = 355 rev/min) as well as mean values of four, that is to say, three central point

3.2 Comparative analysis of the axial drilling force obtained by ANN and regression analysis

The comparative analysis of the values of the axial drilling force F_a obtained by ANN and regression analysis was performed for the following drilling lengths L = 100, 500 and 1000 mm.

The experimental values of the axial drilling force for the drilling lengths L = 100 mm, L = 500 mm and L = 1000 mm are shown in Table 4.

The axial drilling force F_a, as a target function, can be represented in the form of the complex exponentiation, shown by the Eq. 1.

$$F_a = C_F d^{b_1} n^{b_2} s^{b_3} \tag{1}$$

In order to obtain a regression model that describes which will describe the target function as accurately as possible with respect to Eq. 1, the incomplete second-order three-factor model (incomplete quadratic model) with constant coefficients was applied after completion of the linearization, as shown in Eq. 2.

Table 4 The experimental values of the axial drilling force

PLAN-MATRIX													
EXPERI-MENTAL POINTS	Coded values							Actual values			Experimental F_a values [N]		
	X1	X2	X3	X1 X2	X1 X3	X2 X3	X1 X2 X3	d [mm]	n [rpm]	s [mm/rev]	L=100 mm	L=500 mm	L=1000 mm
1	-1	-1	-1	1	1	1	-1	6.0	250	0,027	544,85	649,96	686.90
2	1	-1	-1	-1	-1	1	1	10.0	250	0,027	700,86	996,71	1325.30
3	-1	1	-1	-1	1	-1	1	6.0	500	0,027	401,11	464,31	564.24
4	1	1	-1	1	-1	-1	-1	10	500	0,027	654,23	717,83	768.65
5	-1	-1	1	1	-1	-1	1	6.0	250	0,107	740,32	909,58	959.71
6	1	-1	1	-1	1	-1	-1	10.0	250	0,107	1339,03	1716,27	1907.70
7	-1	1	1	-1	-1	1	-1	6.0	500	0,107	931,98	962,00	989.67
8	1	1	1	1	1	1	1	10.0	500	0,107	1329,16	1531,00	1727.44
9	0	0	0	0	0	0	0	7.75	355	0,053	720,56	838,55	950.36
10	0	0	0	0	0	0	0	7.75	355	0,053	615.73	736.10	870.26
11	0	0	0	0	0	0	0	7.75	355	0,053	633.70	784.84	873.20
12	0	0	0	0	0	0	0	7.75	355	0,053	667,50	703,69	736.60

$$y = b_0 + b_1x_1 + b_2x_2 + b_3x_3 + b_{12}x_1x_2 + b_{13}x_1x_3 + b_{23}x_2x_3 + b_{123}x_1x_2x_3 \quad (2)$$

The coding has been performed by the transformation Eq. 3:

$$x_1 = 2\frac{\ln(D)-\ln(D_{max})}{\ln(D_{max})-\ln(D_{min})} + 1\,, x_2 = 2\frac{\ln(n)-\ln(n_{max})}{\ln(n_{max})-\ln(n_{min})} + 1 \text{ and } x_3 = 2\frac{\ln(s)-\ln(s_{max})}{\ln(s_{max})-\ln(s_{min})} + 1 \quad (3)$$

By applying the regression analysis, the coefficients of models for drilling lengths L =100, 500 and 1000 mm, have been obtained and shown in Table 5.

Based on the coefficients shown in Table 5 and the return to the original coordinates, the regression models of the target function (axial drilling force F_a) were obtained through the transformation Eq. 3. To obtain more accurate results, no verification of the significance of the parameters was performed, and no insignificant parameters were omitted, they were all retained in the model. The equation obtained in this way was used to calculate the values of the axial drilling force F_a. The comparison between results obtained by the ANN simulation and the regression model is shown in Table 6.

Table 5 Coefficients of the regression model

Drilling length	Coefficients of the model							
	b_0	b_1	b_2	b_3	b_{12}	b_{13}	b_{23}	b_{123}
L = 100	6.5943	0.2111	-0.0190	0.3132	-2.52E-05	0.0258235	0.074737	0.0747443
L = 500	6.7604	0.2454	-0.0903	0.2957	-0.02027	0.029545	0.075798	-0.0223
L = 1000	6.8742	0.2763	-0.1012	0.2588	-0.05976	0.034711	0.084119	0.027256

Table 6 Comparative values of the axial drilling force

Drilling length L [mm]	Cutting modes			Results of the experiment F_{eksp} [N]	Results of ANN simulation			Results of Regression analysis		Deviation F_{ANN} from F_{ra} [%]
	d [mm]	n [rpm]	s [mm/rev]		F_{ANN} [N]	Error [%]	ANN	F_{ra} [N]	Error [%]	
L = 100 mm	6.00	500	0.027	401.11	401.06	-0.012	d 21	380.97	-5.021	5.27
	7.75	250	0.027		590.19		d 11	587.07		0.53
	10.00	250	0.107	1339.03	1338.92	-0.008	d 12	1271.80	-5.021	5.28
	6.00	355	0.027		470.51		n 11	443.21		6.16
	7.75	355	0.027		555.65		n 41	533.99		4.06
					560.25		d 51			
	10.00	250	0.053		863.30		s 21	914.04		-5.55
	7.75	355	0.053	659.37 (middle)	646.89	-1.893	s 45	726.43	10.170	-10.95
					690.34	4.697	d 55			
					675.58	2.458	n 45			
L = 500 mm	10.00	500	0.027	717.83	717.86	0.004	d 21	676.18	-5.802	6.16
	10.00	355	0.027		868.87		n 21	795.24		9.26
	6.00	250	0.107	909.58	909.48	-0.011	d 12	856.81	-5.802	6.15
	7.75	250	0.107		1204.08		d 12	1177.71		2.24
	6.00	355	0.107		938.19		n 12	881.44		6.44
	7.75	500	0.053		768.35		s 42	782.88		-1.86
					770.99		d 25			
	7.75	355	0.053	765.80 (middle)	794.40	3.735	s 45	857.34	11.954	-7.34
					808.72	5.605	d 55			
					819.35	6.993	n 45			
L = 1000 mm	10.00	250	0.027	1325.30	1325.28	-0.002	d 11	1248.09	-5.826	6.18
	7.75	500	0.027		680.79		d 21	620.39		9.74
	7.75	355	0.027		813.38		n 41	745.24		9.14
					806.83		d 51			
	6.00	500	0.107	989.67	989.78	0.011	d 22	932.01	-5.826	6.20
	6.00	250	0.053		795.76		s 11	762.02		4.43
	10.00	500	0.053		1101.65		s 22	1076.25		2.36
	7.75	355	0.053	857.61 (middle)	914.19	6.598	s 45	961.28	12.089	-4.90
					905.26	5.557	d 55			
					949.72	10.741	n 45			

The comparison made revealed the following:

- The results obtained by simulation of the ANN at the points of experiment for all drilling lengths are fully are fully consistent with the experimental results with a maximum deviation of less than 0.025 %.
- For controlled drilling lengths (L = 100, 500 and 1000 mm), the maximum deviations of the results obtained by simulation of the ANN in the central plan point, if compared to the experimental results, are:
  - for ANN s45 - 6,598 % at drilling length L = 1000 mm;
  - for ANN d55 - 5.557 % at drilling length L = 1000 mm, and
  - for ANN n45 - 10.741 % at drilling length L = 1000 mm.
- For drilling lengths L = 100, 500 and 1000 mm, the values of the axial force obtained by regression analysis deviate from the experimental results as follows:
  In the points of experiment:
  - 5.022 % for L = 100 mm,
  - 5.802 % for L = 500 mm, and
  - 5.826 % for L = 1000 mm,

  and in the central plan point:
  - 10.17 % for L = 100 mm,
  - 11.954 % for L = 500 mm, and
  - 12.089 % for L = 1000 mm,

  which is significantly less favourable compared to the results obtained by the simulation of ANN.
- The results obtained by simulation of neural networks in the plan points which were not included in the experiment also correspond to the results obtained by regression analysis maximum deviation of less than 9.75 %.

The performed analyses of the results obtained by application of a family of ANNs and their comparison with the experimental results and the results obtained by mathematical modelling of multifactor plans show that prediction of tool condition, in conditions of non-linear dependency of the target function and influential parameters, can be additionally enhanced by application of a family of ANNs. Therefore, a family of ANNs can be applied very successfully in prediction of tool condition, in particular in cases of non-linear dependency of the target function and influential parameters when the regression analysis method fails to render satisfactory results and calls for further experimental research.

4. Conclusion

The prediction of tool condition is of high practical importance, since the (technological and economic) effects of the machining process depend directly on the tool life. However, considering that the machining process is a highly complex physico-chemical mechanism of interaction between tool and workpiece under the conditions of scatter of characteristics and properties of the elements of the technological system, modelling this process seems to be very difficult. The application of modern technologies aimed at solving the problems related to modeling, simulation and monitoring of the machining process has recently begun, and the most commonly used ANNs allow to predict changes in the parameters of interest as a function of changes in the input value.

In this paper the axial cutting force F_a was chosen as a target function, i.e. as a source of information about the amount of cutting tool wear. The influencing factors selected included the material of the tool (twist drill), the sharpening mode, the nominal diameter, the number of revolutions, the feed rate and the drilling length until the twist drills are worn out. Based on the established correlations between the target function and the influencing parameters for predicting the wear size of twist drills, a FANN was developed. The results of the prediction obtained by applying a FANN were compared with the results obtained by regression analysis in the experimental points. The comparison showed that the prediction results were consistent.

Furthermore, the prediction results obtained by applying a FANN deviate significantly less from the experimental results. Therefore, the developed model of FANN can be used as a very reliable method for predicting the state of the tool, especially in case of a nonlinear relationship between the target function and the parameters involved, and in cases where the regression analysis does not give satisfactory results and requires additional experimental research.

References

[1] Spaić, O., Krivokapić, Z., Ivanković R. (2013). Mathematical modelling of cutting force as the most reliable information bearer on cutting tools wearing phenomenon, *Journal of Mechanics Engineering and Automation (JMEA)*, Vol. 3, No. 12, 772-777.

[2] Krivokapić, Z., Zogović, V., Spaić O. (2006). Using neural netvorks to follow the wear of a 390 twist drill, *Strojniški vestnik – Journal of Mechanichal Engineering*, Vol. 52, No. 7-8, 437-442.

[3] Kaya, B., Oysu, C., Ertunc, H.M. (2011). Force-torque based on-line tool wear estimation system for CNC milling of Inconel 718 using neural networks, *Advances in Engineering Software*, Vol. 42, No. 3, 76-84, doi: 10.1016/j.advengsoft.2010.12.002.

[4] Wu, D., Jennings, C., Terpenny, J., Gao, R.X., Kumara, S. (2017). A comparative study on machine learning algorithms for smart manufacturing: Tool wear prediction using random forests, *Journal of Manufacturing Science and Engineering*, Vol. 139, 071018-1-071018-9, doi: 10.1115/1.4036350.

[5] Sekulic, M., Pejic, V., Brezocnik, M., Gostimirović, M., Hadzistevic, M. (2018). Prediction of surface roughness in the ball-end milling process using response surface methodology, genetic algorithms, and grey wolf optimizer algorithm, *Advances in Production Engineering & Management*, Vol. 13, No. 1, 18-30, doi: 10.14743/apem2018.1.270.

[6] Tamang, S.K.; Chandrasekaran, M. (2015). Modeling and optimization of parameters for minimizing surface roughness and tool wear in turning Al/SiCp MMC, using conventional and soft computing techniques, *Advances in Production Engineering & Management*, Vol. 10, No. 2, 59-72, doi: 10.14743/apem2015.2.192.

[7] Neto, F.C., Gerônimo, T.M., Cruz, C.E.D., Aguiar, P.R., Bianchi, E.E.C. (2013). Neural models for predicting hole diameters in drilling processes, *Procedia CIRP*, Vol. 12, 49-54, doi: 10.1016/j.procir.2013.09.010.

[8] Rao, K.V., Murthy, B.S.N., Rao, N.M. (2014). Prediction of cutting tool wear, surface roughness and vibration of work piece in boring of AISI 316 steel with artificial neural network, *Measurement*, Vol. 51, 63-70, doi: 10.1016/j.measurement.2014.01.024.

[9] Martins, C.H.R., Aguiar, P.R., Frech, A., Bianchi, E.C. (2014). Tool condition monitoring of single-point dresser using acoustic emission and neural networks models, *IEEE Transactions on Instrumentation and Measurement*, Vol. 63, No. 3, 667-679, doi: 10.1109/TIM.2013.2281576.

[10] Kannan, T.D.B., Kannan, G.R., Umar, M., Kumar, S.A. (2015). ANN approach for modelling parameters in drilling operation, *Indian Journal of Science and Technology*, Vol. 8, No. 22, doi: 10.17485/ijst/2015/v8i22/79097.

[11] Benkedjouh, T., Medjaher, K. , Zerhouni, N., Rechak, S. (2015). Health assessment and life prediction of cutting tools based on support vector regression, *Journal of Intelligent Manufacturing*, Vol. 26, No. 2, 213-223, doi: 10.1007/s10845-013-0774-6.

[12] Drouillet, C., Karandikar, J., Nath, C. , Journeaux, A.-C., El Mansori, M., Kurfess, T. (2016): Tool life predictions in milling using spindle power with the neural network technique, *Journal of Manufacturing Processes,* Vol 22, 161-168, doi: 10.1016/j.jmapro.2016.03.010.

[13] D'Addona, D.M., Matarazzo, D., de Aguiar, P.R., Bianchi, E.C., Martins, C.H.R. (2016). Neural networks tool condition monitoring in single-point dressing operations, *Procedia CIRP*, Vol. 41, 431-43, doi: org/10.1016/j.procir.2016.01.001.

[14] Patra, K., Jha, A.K., Szalay, T., Ranjan, J., Monostori, L. (2017). Artificial neural network based tool condition monitoring in micro mechanical peck drilling using thrust force signal, Precision Engineering, Vol. 48, 279-291, doi: org/10.1016/j.precisioneng.2016.12.011.

[15] Khorasani¸ A.M., Yazdi, M.R.S. (2017). Development of a dynamic surface roughness monitoring system based on artificial neural networks (ANN) in milling operation, *The International Journal of Advanced Manufacturing Technology*, Vol. 93, 141-151, doi: 10.1007/s00170-015-7922-4.

[16] Mikołajczyk, T., Nowicki, K., Bustillo, A., Yu Pimeno, D. (2018). Predicting tool life in turning operations using neural networks and image processing, *Mechanical Systems and Signal Processing*, Vol. 104, 503-513, doi: 10.1016/j.ymssp.2017.11.022.

[17] Wang, Q., Jia, X. (2020). Multi-objective optimization of CFRP drilling parameters with a hybrid method integrating the ANN, NSGA-II and fuzzy C-means, *Composite Structures,* Vol. 235, 111803, doi: 10.1016/j.compstruct.2019.111803.

[18] Kumar, R., Hynes, N.R.J. (2020). Prediction and optimization of surface roughness in thermal drilling using integrated ANFIS and GA approach, *Engineering Science and Technology, an International Journal*, Vol. 23, Vol. 1, 30-41, doi: 10.1016/j.jestch.2019.04.011.

[19] Mondal, N., Mandal, S., Mandal, M.C. (2020). FPA based optimization of drilling burr using regression analysis and ANN model, *Measurement,* Vol. 152, 107327, doi: 10.1016/j.measurement.2019.107327.

[20] Schorr, S., Möller, M., Heib, J., Bähre, D. (2020). Quality prediction of drilled and reamed bores based on torque measurements and the machine learning method of random forest, *Procedia Manufacturing*, Vol. 48, 894-901, doi: 10.1016/j.promfg.2020.05.127.

[21] Yin, C.P., Wu, Z.P., Dong, Y.W., You, Y.C., Liao, T. (2019). Femtosecond laser helical drilling of nickel-base single-crystal super-alloy: Effect of machining parameters on geometrical characteristics of micro-holes, *Advances in Production Engineering & Management*, Vol. 14, No. 4, 407-420, doi: 10.14743/apem2019.4.337.

[22] Spaić, O. (2017). *Teorija rezanja*, Univerzitet u Istočnom Sarajevu, Fakultet za proizvodnju i menadžment Trebinje, Trebinje, Bosnia and Herzegovina.